Physica E 75 (2016) 309–316

Contents lists available at ScienceDirect

Physica E

journal homepage: www.elsevier.com/locate/physe

Recombination processes in structures with GaN/ALN quantum dots

I.A. Aleksandrov [a,*], V.G. Mansurov [a], K.S. Zhuravlev [a,b]

[a] Rzhanov Institute of Semiconductor Physics, Siberian Branch, Russian Academy of Sciences, 630090 Novosibirsk, Russia
[b] Novosibirsk State University, 630090 Novosibirsk, Russia

HIGHLIGHTS

- Photoluminescence temperature dependence of GaN/AlN quantum dots has been studied.
- Calculated radiative lifetime 1.5 times increases with temperature in 5–300 K range.
- Nonradiative lifetime in GaN QD was calculated in configuration coordinate model.
- Nonradiative recombination of carriers mainly occurs before capture in QDs.

ARTICLE INFO

Article history:
Received 14 July 2015
Received in revised form
28 September 2015
Accepted 1 October 2015
Available online 5 October 2015

PACS:
78.67.Hc
78.47.jd
78.55.Cr
81.07.Ta

Keywords:
Quantum dots
GaN
AlN
Photoluminescence

ABSTRACT

Mechanisms of the generation and the radiative and nonradiative recombination of carriers in structures with GaN quantum dots in the AlN matrix are studied experimentally and theoretically. Absorption, stationary and nonstationary photoluminescence of quantum dots at different temperatures are investigated. It is found that the photoluminescence intensity considerably decreases with the temperature while the photoluminescence kinetics weakly depends on the temperature. The photoluminescence kinetics is shown to be determined by radiative recombination inside quantum dots. A mechanism of nonradiative recombination is proposed, according to which the main reason for the thermal quenching of photoluminescence is nonradiative recombination of charge carriers, generated by optical transitions between quantum dots and wetting layer states.

1. Introduction

GaN quantum dots (QDs) in the AlN matrix are promising for the development of light emitting devices in the visible and UV spectral ranges [1] and high-speed intersubband optical devices operating in the near infrared spectral range [2]. A pronounced physical feature of wurtzite GaN/AlN QDs formed along the (0001) axis is the presence of the built-in extremely strong electric field with a strength of about several MV/cm directed along the (0001) axis. This electric field causes a decrease in the exciton transition energy due to the quantum Stark effect [3] and pushes apart the electron and the hole to the opposite sides of QD, which appreciably increases their lifetimes [3–5].

Large conduction band (1.8 eV) and valence band (0.8 eV) offsets at the GaN/AlN interface [6] lead to a strong localization of charge carriers in QDs, which prevents their capture on the nonradiative recombination centers located in the surrounding matrix. Therefore the structures with GaN/AlN QDs demonstrate a relatively small decrease in the PL intensity with an increase in the temperature as compared to QDs based on narrow-band materials and GaN/AlN quantum wells [7–9]. The studies performed in [5,8–10] show that the PL intensity ratios of QDs at room and helium temperatures (I_5/I_{300}) are 0.3–0.8 [9], 0.62 [10], ~0.3 [5], and ~0.5 [8]. The activation energies of the QD PL quenching are usually about several tens of meV [9,11], which is 10–100 times lower than the escape energies of charge carriers from QDs to the wetting layer and the matrix. The temperature quenching of the PL intensity can be caused by thermally induced tunneling of charge carriers from QDs to nonradiative recombination centers in the matrix [5,11], nonradiative recombination of charge carriers in the wetting layer (WL) [9], and Auger recombination in QDs [12].

* Corresponding author. Fax: +7 3833332771.
E-mail address: aleksandrov@isp.nsc.ru (I.A. Aleksandrov).

http://dx.doi.org/10.1016/j.physe.2015.10.004
1386-9477/

Theory taking into account all these processes has not been proposed so far.

Another feature of GaN/AlN QDs is a weak decrease in the lifetime of charge carriers in comparison with a decrease in the PL intensity with an increase in the temperature [8,5]. This can be due to both increase in the radiative lifetime with the temperature [5] and nonradiative losses before the capture of charge carriers in QDs [8]. Theoretical calculations of the temperature dependence of the radiative and nonradiative lifetimes in GaN/AlN QDs have not yet been performed. Furthermore, in [9] the nonradiative losses in the WL were considered to be negligible, however, as shown in this work, it is necessary to take them into account for the consistent description of the temperature dependence of the luminescence intensity and the lifetime.

In this work we considered various mechanisms of the charge carrier generation in the structure with QDs under optical excitation: absorption inside QDs, absorption in the WL, and absorption during the transitions between the WL and QD states. Possible mechanisms of nonradiative recombination (tunneling of charge carriers from QDs to the nonradiative recombination centers, thermal emission of charge carriers from QDs to the matrix or to the WL followed by nonradiative recombination on defects, Auger recombination in QDs, nonradiative recombination of carriers generated in the WL and in the matrix) were analyzed. In order to determine the relative contribution of these mechanisms the temperature dependence of stationary and nonstationary PL of structures with QDs was examined and the obtained results were compared with the calculated data.

2. Experimental details

Structures with GaN QDs in the AlN matrix were grown by molecular beam epitaxy in a Riber CBE-32 system, using ammonia as a nitrogen source. The structures were grown on sapphire substrates along the (0001) direction. The structures consist of an AlN buffer layer with a thickness of 150 nm and ten GaN QD layers covered by 10 nm-thick AlN layers. The structures were grown at a substrate temperature of 900 °C. The nominal amount of deposited GaN evaluated by the growth rate of GaN layers was 15, 7.5, and 3 monolayers for the samples labeled as A, B, and C, respectively. The QD formation was controlled during the growth by high-energy electron diffraction [13].

Fig. 1 depicts a TEM image of QDs in a typical sample (sample B). In this sample the average QD height (h_{QD}) is 3.4 nm, the average QD diameter (d_{QD}) is 14 nm, the average WL thickness (h_{WL}) is 0.8 nm, and the QD density is 1.5×10^{11} cm^{-2}. More detailed data on the QD size distribution are given in [14]. The average QD height, diameter, and QD density were estimated as 2.9 and 3.6 nm, 12 and 15 nm, and 10^{10} cm^{-2} and 3.5×10^{11} cm^{-2} for samples C and A, respectively. The dislocation density was 5×10^{10} cm^{-2} for samples B and C and 5×10^{11} cm^{-2} for sample A, as obtained from the plan-view TEM images.

Continuous He–Cd laser ($\hbar\omega$ = 3.81 eV), pulsed nitrogen laser ($\hbar\omega$ = 3.68 eV), and pulsed Nd:YLF laser ($\hbar\omega$ = 4.71 eV) were applied for PL excitation. A He–Cd laser spot diameter was about 0.5 mm. The repetition rate of N_2 laser pulses was 1 kHz; the pulse duration was 7 ns; the laser spot diameter was about 1 mm. The repetition rate of Nd:YLF laser pulses was 1 kHz; the pulse duration was 3 ns; and the laser spot diameter was about 0.5 mm. According to our previous studies [14], the excitation power was selected so that to provide the generation of no more than one electron–hole pair in QD and was 5 mW for the He–Cd laser, 0.034 mW for the N_2 laser, and 0.08 mW for the Nd:YLF laser. Luminescent radiation was analyzed by a double diffraction monochromator and detected by a cooled photomultiplier with an S-20 photocathode. PL decay curves were measured by a time-correlated single photon counting system. The sample temperature was varied in the range of 5–300 K using a helium cryostat; the accuracy of temperature set and maintenance was ± 1 °C. To measure the absorption spectra a spectrophotometer with a deuterium lamp as a radiation source was used. The measured absorbance of the structure with QDs is proportional to $\alpha_{AlN} d + (K_{WL} + \sigma_{QD} n_{QD}) N$, where α_{AlN} is the AlN absorption coefficient, d is the total thickness of AlN layers, K_{WL} is the WL absorption loss coefficient, σ_{QD} is the QD absorption cross-section, n_{QD} is the QD density, and N is the number of QD layers.

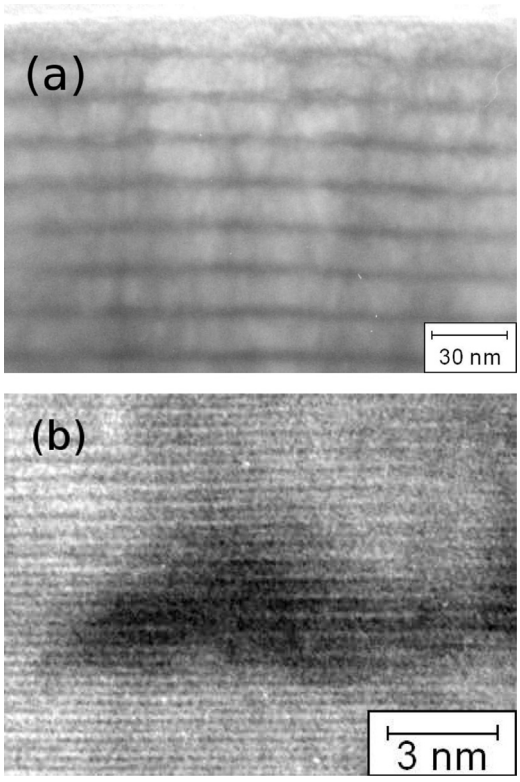

Fig. 1. Cross-section TEM images of the GaN structure with QDs in the AlN matrix (sample): (a) in the bright field mode and (b) in the high resolution mode showing a single QD.

3. Results

Fig. 2a depicts the light absorption spectrum of sample B measured at room temperature. From the figure it is seen that the absorption coefficient increases with the energy in the range $\hbar\omega$ = 3.5–5.3 eV. At $\hbar\omega$ = 5.3 eV a local maximum is observed, then there is a small decrease in the range $\hbar\omega$ = 5.3–5.6 eV, after which the absorption coefficient increases in the range $\hbar\omega$ = 5.6–6.1 eV. A sharp increase above 5.9 eV corresponds to the band-to-band absorption in the AlN matrix.

Fig. 2 b presents the energy diagrams of QDs and the WL with sizes of h_{QD}=3.4 nm and h_{WL}=0.8 nm corresponding to the average QD height and WL thickness in sample B, which were calculated in the $\mathbf{k}\cdot\mathbf{p}6\times6$ approximation using the nextnano++ simulation tool [15]. In the calculation GaN and AlN parameters from [14], GaN and AlN valence band parameters from [16] were used. It was assumed that QDs had a shape of a hexagonal truncated pyramid located at the WL. The figure also shows the QD and WL ground state energy levels, optical transitions in QDs, the WL, and between the QD and WL states. The crossing transitions between the QD and WL states were previously observed in the